

Supplementary Materials

S1: Modeling Approaches

The foundation of the modeling for this effort was species distribution models (SDMs), based largely on climatic-niche envelopes. SDMs allowed us to produce habitat suitability maps which we used to identify core habitat areas, assess landscape resistance for connectivity modeling, and assign patch values for metapopulation modeling. We developed ensemble SDMs for each focal species under historic conditions and then projected suitability, connectivity, and metapopulation persistence under four future climate scenarios to determine how and where connectivity may be able to help support persistence of biodiversity in the south coast ecoregion.

1.1 Ensemble Species Distribution Modeling

We used SDMs to predict the distribution of suitable habitat for our five focal species representing different habitat associations: mountain-conifer dependent spotted owl, shrub-dependent wrentit, chaparral-dependent big-eared woodrat, riparian-dependent western toad, and the long-distance dispersing, generalist bobcat.

1.1.1 Occurrence Data

For all focal species, we mined public databases (*e.g.*, eBird, iNaturalist, BIOS) and all unpublished literature for presence points for each species to obtain adequate sample sizes and geographic coverage across the study area (Table S1). To avoid including older data points in areas that have since been developed (thus artificially suggesting urban areas may be suitable based on these locations), we implemented a temporal cutoff, only using data from 1980 to present. We also filtered data so only locations with an accuracy of 500 m or better were retained.

In contrast to data collected as part of a thoughtful and thorough sampling regime, opportunistic data are subject to sampling bias. This sampling bias often results in inadequate representation of the environmental space, which leads to environmental bias in SDM model results and inaccurate model predictions [1]. To address sampling bias, we spatially restricted the sampling of background points when absence points were not available.

The data for big-eared woodrat, bobcat, and western toad required the selection of pseudo-absence or background points. From a visual inspection of the presence points for big-eared woodrat and bobcat, it appeared they were heavily biased toward primary and secondary roads in the study area. We confirmed this bias by sampling the presence points on a distance from roads surface. We counted the number of presence points within each 500 m distance from roads bin and randomly sampled the same number of background points in each distance from roads bin, generating a 3:1 ratio with the presence points for each species. This ratio of absence and pseudoabsence to presence points was selected to help maximize the differentiation between suitable and unsuitable habitat [2] while using a consistent approach across the different models we employed for our ensemble SDMs [3]. Because western toad data were often gathered during stream surveys, they did not appear to be biased towards roads, and therefore, we did not bias the generation of background points for this species. For all three of these species, there was often a disparity in the distribution of occurrence points that was likely due to bias in sampling effort. With coordinated research and monitoring efforts focused in the coastal regions in San Diego, Orange, western Riverside, and Los Angeles Counties within our study region, these areas often had more data readily available on public databases. As such, we found model performance improved both quantitatively and qualitatively when we split the study area to address effort or reporting bias, generating a relative number of background points to occurrence points on a subregional basis.

Table S1. List of focal species selected for modeling with data sources identified. The number of occurrence points available and the number and type points (background or true absence) used in species distribution modeling for each species.

| Focal species (<i>Scientific name</i>) | Habitat association | Data sources | # presence points | Absence or background points | # absence/ background points |
|---|---|--|----------------------|------------------------------------|------------------------------------|
| California spotted owl (<i>Strix occidentalis occidentalis</i>) | Coniferous and hardwood forest | eBird ¹ , CNDDDB ² | 1865 | Absence | 5595 |
| Wrentit (<i>Chamaea fasciata</i>) | Shrubland | eBird ¹ | 5894 | Absence | 17,682 |
| Western toad (<i>Anaxyrus boreas</i>) | Riparian, wetland, and upland scrub | GBIF ³ , BISON ⁴ , USFS ⁵ , USGS ⁶ NAHerp ⁷ , HerpMapper ⁸ | 1029 | Background | 3087 |
| Bobcat (<i>Lynx rufus</i>) | Generalist | GBIF ⁹ , BISON ⁴ , Arctos ¹⁰ , NPS-SAMO ¹¹ , SDNHM ¹² , USFS ⁵ , SDSU ¹³ | 507 | Background | 1521 |
| Big-eared woodrat (<i>Neotoma macrotis</i>) | Chaparral | GBIF ¹⁴ , BISON ⁴ , SDNHM ¹² , VertNet ¹⁵ | 473 | Background | 1419 |

¹[4]; ²California Natural Diversity Database [5]; ³Global Biodiversity Information Facility [6]; ⁴Biodiversity Information Serving our Nation [7]; ⁵United States Forest Service [8]; ⁶United States Geological Survey (R.N. Fisher, *unpublished data*); ⁷[9]; ⁸[10]; ⁹[11]; ¹⁰[12]; ¹¹National Park Service-Santa Monica Mountains (S.P.D. Riley, *unpublished data*); ¹²San Diego Natural History Museum [13]; ¹³San Diego State University [14]; ¹⁴[15]; ¹⁵[16].

Because the eBIRD database contains actual absence points in the form of observation locations where species are not seen, we were able to use these absences for modeling of the wrentit and California spotted owl. We randomly selected absence points to use in our modeling of wrentit and California spotted owl at a ratio of 3:1. We assumed absence locations to have the same sampling bias as presence locations and therefore did not spatially restrict absence points like we did for the other species.

1.1.2 Species Distribution Modeling

There are many models considered appropriate for analyzing presence-background data — all with various advantages and disadvantages [17,18]. As such, using multiple models to produce a final ‘ensemble’ model has been proposed as the optimal way to estimate presence-background models [19]. Ensemble models have been shown to produce more robust predictions and to perform better than any single model [19,20].

We selected two regression methods (Generalized Linear Models [GLMs]; Generalized Additive Models [GAMs]) and three machine-learning methods (Random Forests [RF]; Boosted Regression Trees [BRT]; MaxEnt) for our suite of SDM models. We implemented all models in R [21], using the *biomod2* package [22] for random forest, boosted regression, and generalized linear models, MaxEnt in the *dismo* package version 1.1-4 [23], and generalized additive models using the *mgcv* package [24]. We elected to generate GAMs and MaxEnt in alternate packages to more readily specify the parameters in those modeling approaches that can affect modeling outputs. We performed a 10-fold cross validation procedure for all

models to assess model predictive ability. Across the 10 folds, we calculated the area under the receiver operating characteristic curve (AUC), and used this as our model performance metric. We also tested the true skill statistic (TSS) as an evaluation metric for our initial models as AUC has been criticized for, among other reasons, ignoring predicted probability and biases related to absence distribution [25]. However, we found that both metrics were closely correlated, consistent with findings of prior research [26], so proceeded with additional modeling steps using AUC.

We computed AUC-weighted ensemble suitability predictions, discarding models with $AUC < 0.7$. We used the final ensemble model for each species to predict habitat suitability across the study area and to generate the predictions under the four future scenarios. The bootstrapped accuracy averaged across ten subsamples of data for each of the five models was 0.95 for owls, 0.80 for wrentit, 0.85 for woodrat, 0.83 for Western toad, and 0.80 for bobcat. To project the distribution of future suitable habitat, we substituted future climate variables into the ensemble models. The data, models and final suitability estimates for each species were reviewed, discussed with, and corroborated by local species-specific experts, and all models were quantitatively evaluated using cross-validation based on prediction of presence versus absence for withheld testing data.

Using the SDM suitability in the historic and future (2100) time periods as end points, we interpolated suitability at annual time steps in the intervening years. We then used these surfaces to generate resistance surfaces for the decadal connectivity modeling, define habitat patches for linkage and metapopulation modeling, and estimate carrying capacities of metapopulation patches.

1.1.3 Patch Maps

For both the least cost corridor linkage modeling and the metapopulation model construction, maps of habitat patches must be established. For each year that was modeled or interpolated, we generated habitat suitability maps that assign a continuous suitability value, ranging from 0 to 1, to each cell within the study area. To translate continuous suitability metrics to discrete habitat patches, we used the Core Mapper functionality in the Gnarly Landscape Utilities toolbox [27]. Core Mapper works by selecting patches that meet three criteria: a minimum per-pixel suitability threshold, an average minimum suitability threshold within a specified moving window, and a minimum core area size threshold, which can be thought of as the area needed to allow for enough territories to have a viable population. With these parameters specified for each species (Table S2), Core Mapper identifies aggregations of suitable grid cells that serve as self-sustaining population cores. The network of these cores represents the meta-population within the study area. For each species, we ran Core Mapper for every time step, retaining suitability values within the core, and setting values outside the cores to zero.

Table S2. Core Mapper input values used to designate patches of core habitat for each focal species.

| | Moving Window Radius (m) | Min Average Habitat Value | Minimum Habitat Value Per Pixel | Min Core Area size (km²) |
|-----------------------------------|---|--------------------------------------|--|--|
| Big-eared woodrat | 422 | 0.45 | 0.25 | 4 |
| Bobcat | 1260 | 0.35 | 0.15 | 25 |
| California spotted owl | 1000 | 0.5 | 0.25 | 20 |
| Wrentit | 800 | 0.6 | 0.314 | 1 |
| Western toad | 232 | 0.55 | 0.343 | 4 |

1.2 Linkage Modeling

1.2.1 Least Cost Corridor Modeling

Habitat patch layers (described above) and resistance were used as the primary inputs for the least cost corridor linkage modeling we performed for decadal time steps under each scenario. Recent studies on large mammals and birds have found habitat use was not linearly related to resistance and that individuals are more tolerant of sub-par environmental features when dispersing than when occupying territories or home ranges (e.g., [28-30]). To account for this possibility we used a non-linear transformation to transform the habitat suitability values to resistance [28]. Resistance was calculated from the following formula:

$$resistance = 100 - 99 * ((1 - \exp(-c * habitat\ suitability)) / (1 - \exp(-c))) \quad (1)$$

where we set $c = 2$ for big-eared woodrat, $c = 4$ for bobcat, $c = 4$ for California spotted owl, $c = 0.25$ for wrentit, and $c = 2$ for western toad.

We ran Linkage Mapper using both the cost-weighted and Euclidean adjacency methods, and removing linkages that run through core areas. After generating the least cost corridors and mosaicking them into a single map, we then reviewed the outputs for each species for the historic period to determine an appropriate cut off of the least cost corridor distance to apply for final delineation of the linkage network for each species. Once we selected the maximum normalized least cost corridor distance for each species (60 km for big-eared woodrat, 60 km for bobcat, 100 km for California spotted owl, 40 km for western toad, and 40 km for wrentit), we applied this cut off to all future scenarios as well. We did not apply species-specific dispersal limitations at this stage so as to allow for corridors to be developed that would accommodate species with similar habitat associations but not necessarily the same dispersal limitations. Instead, species-specific dispersal was integrated into the population models to assess functional connectivity and biological importance of each linkage.

1.2.2 Circuitscape Linkages

We followed our least cost corridor modeling with Circuitscape modeling implemented in Julia 0.7 to determine if any linkage zones were underrepresented strictly based on modeling approach. Due to computational limitations, we only performed this process for the historic condition and within the ecoregion, not the extended study area (Figure 1). We rescaled our resistance surfaces by a factor of three, producing a 270-m resistance surface for modeling. We generated source points across the study area by probabilistically sampling 1000 points on the historic habitat suitability surface for each species. This sampling results in more points being placed in areas with higher habitat suitability than lower suitability. Circuitscape was run in pairwise mode and once cumulative current maps were produced for each species, we rescaled them from 1-100 and combined those surfaces across focal species. We generated a maximum current map by compiling the highest valued pixels for any given species, and an average current map by averaging the value for each pixel across all five species. We thresholded each of these surfaces, the maximum at > 70 and the average at > 80 , and used each of these outputs to compare to the multispecies linkage map and fill gaps.

1.2.3 Land Facet Linkages

In addition to the focal species linkages, we also generated corridors using a species-agnostic landscape approach focused on geodiversity [31,32], or land facets [33,34], designed to identify linkages that retain a range of features defined by slope angle, solar insolation, topography, and elevation. This method was specifically developed as an approach to connectivity assessments under climate change that would be robust to the uncertainty in climate data and issues with scale. To execute the land facet modeling,

we used ecologically-relevant landform data [32] as the source for the individual facets. Of the 15 landforms in the original dataset, we selected three representing cool landforms (cool lower slopes, cool upper slopes, and cool peaks and ridges) and two to represent grasslands (valley and narrow valley), which we were not able to incorporate with our focal species. To generate land facet linkages, we conducted our analysis as described in the Land Facet Corridor Designer User Guide [35] using the Land Facet Corridor Designer [36] and Linkage Mapper [37] toolboxes in ArcGIS.

We identified the areas of greatest density of each of the new landforms using the Calculate Density Surface tool in the Land Facet Corridor Designer toolbox by inputting each of the individual variables used to create the landforms: slope position (ridges/peaks, upper slopes, lower slopes, and valley bottoms), topographic position index (TPI), slope, and continuous heat load index (CHILI). That output was then used to generate termini polygons of the areas of greatest density of each land facet within our conserved areas. We also used the land facet density surface to create a Mahalanobis distance raster for each class of the land facet raster to be used in our corridor modeling as the equivalent of resistance. To standardize the scale of the Mahalanobis distance raster, we used the Chi Square Raster Transform tool. This creates a resistance or distance surface (on a 0 to 1 scale) to use in our corridor modeling where cells with a greater distance (closer to 1) from an area of high density of the land facet of interest have a higher resistance value. Finally, because the surfaces created thus far only include topographic variables and have not incorporated any other landscape features that may affect wildlife movement, we clipped this resistance layer using an urban raster mask generated from land-use data from the Southern California Association of Governments to exclude urban areas from our corridor modeling.

We used Linkage Mapper [37] to generate least cost corridors using the Mahalanobis distance surfaces as our resistance inputs and the termini polygons of high land facet density within large blocks of conserved lands as our target core areas to connect. This process generated raster corridor surfaces that can then be truncated to identify corridor extent. We selected cutoff values for each land facet raster that produced a contiguous corridor but was not too wide or expansive. We examined the final land facet corridors to identify unique corridors that had not been captured by our multispecies linkage and found that only valleys and narrow valleys were not already captured by our final multispecies linkage network.

1.3 Metapopulation Modeling

For the metapopulation component of our modeling approach, SDM predictions of habitat suitability defined the carrying capacities of metapopulation patches, and a demographic model determined the population dynamics within and across the patches. Each model simulation lasted 100 years, meant to represent the time horizon 2000-2100. We generated models for each species under a no-change scenario, as well as the warmer, wetter (CNRM-CM5) and hotter, drier (MIROC5) climate predictions under business as usual emissions (RCP 8.5). To implement metapopulation modeling, we first input our core maps into the software package RAMAS GIS® 5.0 [38] to link the time series of maps to the population model. RAMAS translates the suitability values within a pixel, summed across a core, to the carrying capacity of a population patch. We set initial abundances to some fraction (0.6-1) of the total carrying capacity. Each annual core and suitability map was input into RAMAS to allow population patches to grow or sink in size, changing the overall carrying capacities along with dispersal distances between patches. In addition to the carrying capacity changes due to climate-driven changes in suitability, we imposed random fluctuations (approximately 15% for bobcat and owls, 30% for Western toad, 40% for wrentit, and there were no fluctuations in the carrying capacity of woodrat) in the carrying capacity meant to reflect environmental stochasticity.

Once corridors were identified for each species, they were also integrated into metapopulation models. These models assumed that individuals were well-mixed within a patch and that distances between patches evolved with climate change. We considered the importance of existing corridors only and the

amount of dispersal through linkages was dependent on species' ability, abundance of the giving patch, and carrying capacity of the final patch.

1.3.1 Demographic model

For spotted owl, wrentit, western toad, and bobcat we began with vital rates identified in COMADRE [39] and adjusted them to account for errors (spotted owl) and local conditions (wrentit, western toad, and bobcat) using local data sources provided by species experts we consulted. For woodrat we used a model developed by Stephen Rice (personal communication) that calculated survival and fecundity rates using survival and matrilineal data from [40-42]. In a given year, each individual of a species either lives or dies with or without replacement subject to the typical matrix model equation:

$$\begin{bmatrix} n_1(t+1) \\ n_2(t+1) \\ n_3(t+1) \\ \vdots \\ n_w(t+1) \end{bmatrix} = \begin{bmatrix} f_1(t) & f_2(t) & \dots & f_{w-1}(t) & f_w(t) \\ s_1(t) & r_2(t) & \dots & 0 & 0 \\ 0 & s_2(t) & \dots & 0 & 0 \\ \vdots & \vdots & \ddots & \vdots & \vdots \\ 0 & 0 & \dots & s_{w-1}(t) & s_w(t) \end{bmatrix} \begin{bmatrix} n_1(t) \\ n_2(t) \\ n_3(t) \\ \vdots \\ n_w(t) \end{bmatrix} \quad (2)$$

Here $f_i(t)$, $s_i(t)$, $r_i(t)$, and $n_i(t)$ are the fecundities, survivals, survival-at-same-stage, and numbers of individuals, respectively, for each of the w stages (wrentit and woodrat models had $w = 2$ stages, bobcat had three gender-specified stages, western toad also had three stages, and spotted owl had four stages). Only the western toad had non-zero $r_i(t)$, which means that an individual could remain a juvenile between years. Fecundity and survival are drawn each year from a distribution with specified mean and standard deviation. Thus, vital rates were meant to represent an additional source environmental stochasticity. To incorporate demographic stochasticity, vital rates for each individual were drawn from a Poisson distribution (for fecundities) or a multinomial distribution (for transition rates). Final mean vital rates used in the demographic models for each species are listed in Table S3.

1.3.2 Catastrophes

For wrentit and owl, we added local (within population, not across population) catastrophic drought that decreased vital rates in a given time step. Droughts were assumed to occur every 4-5 years, which is less than California's historic drought frequency, but consistent with species response frequency. We imposed periodic drought because the impact of drought on vital rates has been documented in the literature [43,44]. We did not include a drought catastrophe in the metapopulation modeling for bobcat or woodrat as we did not have empirical data to determine if or how drought might negatively impact the vital rates of these species. For the western toad, although we would expect this species to be negatively impacted by drought, incorporating this catastrophe into the metapopulation modeling led to high instability in abundance, making the identification of priority corridors impossible. We therefore omitted drought catastrophes in the population modeling for this species as well.

We tested the importance of each linkage by comparing the final abundance of the metapopulation with each corridor activated individually and compared that to models where no corridors were active. We used the change in final abundance to calculate the percent increase in the metapopulation when the corridor was added, which we called 'improvement by addition'. To focus on biologically important changes in landscape connectivity, we determined a minimum threshold above which we did not expect changes in final population size were due to chance alone. Finally, we rescaled the percent increase in abundance calculated for each corridor into a relative importance metric ranging from 0 to 1 based on the minimum threshold and the maximum percent increase observed across all scenarios. This threshold was especially important given all the sources of variability in the model.

Table S3. Mean vital rates for each species used in metapopulation models.

Big-eared woodrat

| | Juvenile | Adult |
|----------|----------|--------|
| Juvenile | 0.3145 | 1.2113 |
| Adult | 0.3631 | 0.7125 |

Bobcat

| | Female Kitten | Female Yearling | Female Adult | Male Kitten | Male Yearling | Male Adult |
|--------------|---------------|-----------------|--------------|-------------|---------------|------------|
| Female Kit | 0 | 0.532 | 1.125 | 0 | 0 | 0 |
| Female Year | 0.6 | 0 | 0 | 0 | 0 | 0 |
| Female Adult | 0 | 0.681 | 0.769 | 0 | 0 | 0 |
| Male Kit | 0 | 0.532 | 1.125 | 0 | 0 | 0 |
| Male Year | 0 | 0 | 0 | 0.6 | 0 | 0 |
| Male Adult | 0 | 0 | 0 | 0 | 0.681 | 0.769 |

California spotted owl

| | Juvenile | Subadult 1 | Subadult 2 | Adult |
|-----------|----------|------------|------------|-------|
| Juvenile | 0 | 0.2 | 0.2 | 0.4 |
| Subadult1 | 0.7 | 0 | 0 | 0 |
| Subadult2 | 0 | 0.7 | 0 | 0 |
| Adult | 0 | 0 | 0.9 | 0.8 |

Western Toad

| | Pre-juvenile | Juvenile | Adult |
|--------------|--------------|----------|-------|
| Pre-juvenile | 0 | 50.5 | 1404 |
| Juvenile | 0.086 | 0.21 | 0 |
| Adult | 0 | 0.11 | 0.78 |

Wrentit

| | Juvenile | Adult |
|----------|----------|-------|
| Juvenile | 0.615 | 1.14 |
| Adult | 0.424 | 0.742 |

1.3.3 Corridors and Dispersal

Once least cost corridors had been identified, they had to be integrated into the population model. Combining the spatial corridor identification offered by Linkage Mapper and the evolution of edge-to-edge distances provided by RAMAS was non-trivial. This required updating the permissible corridors every decade so that RAMAS would not allow flow of individuals between areas where the Euclidean distance was short but the cost distance was prohibitive. Regardless, the RAMAS population modeling framework is agnostic with respect to how an individual disperses between patches, and only cares about the amount that flows through patches. We made dispersal proportional to the time-evolving edge-to-edge distances

between patches. We set the mean dispersal distance to 0.5 km for wrentits [45], 25 km for owls [46], 1.5 km for woodrats [47] 1.5 km for western toad [48], and 18 km for bobcats [14]; maximum dispersal distance was designated as 2 km for wrentits, was 150 km for owls, was 3 km for woodrats, 3 km for western toad, and 50 km for bobcats.

Owls had exponentially declining dispersal with distance based on the shape of the dispersal curve at distances above 10 km in [46] (10 km is roughly the radius of a larger non-breeding territories in Oregon, where the study was conducted). Bobcats also had exponentially declining dispersal with distance. For the remainder of the species, dispersal declined exponentially with the square of the distance between patches. This created more dispersal between closely spaced patches, and more overall dispersal given the imposition of the maximum dispersal distance. In addition, we fixed dispersal between any two patches such that less than 10% of individuals in the giving patch went to any one adjacent patch, the fraction of individuals dispersing was a linear function of the number of individuals in the giving patch, and the fraction of individuals dispersing was a linear function of the carrying capacity of the receiving patch up to a threshold (typically around 100 individuals), where the threshold was defined by sensitivity tests to maximize the benefit of dispersal in the no change scenario.

1.3.4 Connectivity Scenarios

For each of the identified corridors, we ran a population model in the presence of the corridor and no other corridors, and in the absence of the corridor with all other corridors active. We then compared the final abundance from each perspective to the final abundances of models with no dispersal and with full dispersal, respectively, to calculate the percent increase in the metapopulation when the corridor was added and % decrease when it was taken away. The results from these two perspectives largely mirrored each other, with some situations where a corridor was important in isolation, but redundant when removed from an otherwise fully connected landscape.

Finally, we ran trials to determine a threshold above which we thought that observed changes in corridor scenarios were due to the influence of a corridor and not due to random fluctuations in the stochastic models. This threshold was especially important given all the sources of stochasticity in the model: sampling births and deaths in a small population (i.e., demographic stochasticity), year-to-year variability in vital rates, year-to-year variability in carrying capacity, and local catastrophes. By creating a system where reorganization of individuals between patches minimizes the impacts of environmental fluctuations, we created a model that maximizes the benefits of connectivity.

S2: Prioritization for Multispecies Linkage Assembly

2.1 Within-species Prioritization

Given the scale and scope of the project, prioritization was critical to achieve a realistic and implementable multispecies linkage network. Our prioritization was based on inputs from four main categories (Figure S1; described in more detail below):

- conservation feasibility,
- connectivity/landscape value,
- climatic consensus value,
- metapopulation persistence (which incorporates species-specific dispersal limitations)

The climatic consensus metrics allowed us to assign greater value to areas where there was agreement about important linkages over time and across scenarios, providing greater support for decision-making under uncertainty. In contrast, by combining currently known landscape conditions such as impervious surface cover and percent land conserved with those that are less certain from our climatic modeling, our

prioritization approach was grounded in empirical data while providing a robust framework for considering the value of linkages in the future for resilience in the face of climate change.

Specifically, we developed the priority linkage value for a patch using the Environmental Evaluation Management System (EEMS 2.02; [49]), a hierarchical decision-making toolbox in ArcGIS (ESRI, Redlands, CA) based on fuzzy logic described in the main text. We implemented this prioritization according to the following procedure:

Step 1: After fuzzifying initial input variables as described in Table S4 and S5, we calculated intermediate values for several metrics to combine or select among them, as appropriate.

- *Habitat Quality* was calculated by taking the EEMS Union (the mean of all inputs) of the fuzzified values of impervious cover, patch shape, and the habitat resistance values.
- *Network Connectivity* was calculated by taking the EEMS union of the fuzzified centrality and betweenness values.
- *Prior Designation* was calculated by taking the EEMS OR (the larger fuzzified value of the two inputs) of the proportion overlap with either the South Coast Missing Linkages (SCML) corridors or the California Essential Habitats Connectivity (CEHC) linkages.
- *Conservation Feasibility* was calculated by taking the EEMS selected union (the mean of the 2 largest of the inputs) of the parcels per patch, proportion already conserved and the average parcel size.
- *Climate Consensus* was calculated by first taking the larger of CNRM-CM5 RCP 8.5 linkage accounting between 2010 and 2100 or the connection to analogous conditions under the same scenario using climatic water deficit. We applied the same selection to the MIROC5 RCP 8.5 linkage accounting and connectivity to analogous conditions. Finally, we combined the selected value from each of these scenarios and combined them with the linkage accounting for the CNRM-CM5 RCP 4.5 and MIROC5 RCP 4.5 scenarios using an EEMS union.
- *Metapopulation Persistence* was an EEMS union of the metapopulation priority values under three different climate scenarios, No Change, CNRM-CM5 RCP 8.5 and MIROC5 RCP 8.5. For one of our species, the spotted owl, we also added a Vegetation Vulnerability scenario.

Step 2: We combined some of the intermediate values further.

The *Connected Landscape* value was then obtained by taking the EEMS SELECTED UNION (the mean of the 2 largest of the inputs) of *Habitat Quality*, *Network Connectivity*, and *Prior Designation*.

Step 3: *Connected Landscape*, *Conservation Feasibility*, *Climate Consensus* and *Metapopulation Persistence* values were combined in an EEMS UNION.

Step 4: The result of step 3 was combined with impervious cover in an EEMS AND which returns the smaller of the two inputs to ensure linkage segments that had a high degree of impervious surface (*i.e.*, urbanization) would be downgraded given the difficulty in restoring connectivity in these areas. This final value was the **Within-species Linkage Priority** value for each core and linkage segment.

Table S4. Range and mean of input values for EEMS prioritization metrics by category. The range and mean of the fuzzy values of each metric are also listed. Fuzzy conversion functions either convert linearly between the false and true threshold or along a curve following set points between the false and true thresholds.

| Metric | Original scale | Original mean | Fuzzy conversion function | Conversion thresholds (false – true) | Fuzzy scale (false – true) | Fuzzy mean |
|-------------------------------------|----------------|---------------|---------------------------|--------------------------------------|----------------------------|------------|
| Conservation feasibility | | | | | | |
| # Parcels/Area | 0 – 0.61 | 0.39 | linear | 0.576 – 0.0006 | -1 – 1 | -0.35 |
| Average parcel size (ha) | 0 – 5.59 | 1.4 | linear | 0 – 5.59 | -1 – 1 | -0.106 |
| Proportion conserved | 0 – 1.0 | 0.38 | linear | 0 – 0.99 | -1 – 1 | -0.22 |
| Connectivity/landscape value | | | | | | |
| % Imperviousness | 0 – 57.59 | 16.29 | linear | 33.92 – 2.1 | -1 – 1 | 0.22 |
| Patch shape | 0 – 1.1 | 0.03 | linear | 1.1 – 0.0018 | -1 – 1 | 0.822 |
| Resistance | 47.98 – 77.69 | 56.95 | linear | 72.06 – 52.27 | -1 – 1 | 0.54 |
| Centrality | 1 – 13 | 3.72 | linear | 1 – 8 | -1 – 1 | -0.32 |
| Betweenness (log) | -4.61 – 8.25 | 1.77 | linear | -4.61 – 8.25 | -1 – 1 | 0.36 |
| Prop overlap - SCML | 0 – 0.93 | 0.13 | curve | 0,-1; 0.3,0.5; 0.8,1 | -1 – 1 | -0.5 |
| Prop overlap - CEHC | 0 – 1 | 0.33 | curve | 0,-1; 0.3,0.5; 0.8,1 | -1 – 1 | -0.04 |
| Climate consensus | | | | | | |
| Linkage value CNRM-CM5, RCP 4.5 | 0 – 1 | 0.65 | curve | 0.1,-1; 0.3,0.5; 0.5,0.8 | -1 – 0.8 | 0.67 |
| Linkage value CNRM-CM5, RCP 8.5 | 0.09 – 1 | 0.63 | curve | 0.1,-1; 0.3,0.5; 0.5,0.8 | -1 – 0.8 | 0.63 |
| CNRM-CM5 RCP 8.5 analog | 0.37 – 1 | 0.76 | linear | 0 – 0.8 | -0.07 – 1 | 0.83 |
| Linkage value MIROC5, RCP 4.5 | 0.05 – 1 | 0.59 | curve | 0.1,-1; 0.3,0.5; 0.5,0.8 | -1 – 0.8 | 0.56 |
| MIROC5 RCP 8.5 analog | 0.34 – 1 | 0.75 | linear | 0 – 0.8 | -0.15 – 1 | 0.81 |
| Linkage value MIROC5, RCP 8.5 | 0 – 1 | 0.59 | curve | 0.1,-1; 0.3,0.5; 0.5,0.8 | -1 – 0.8 | 0.51 |
| Metapopulation persistence | | | | | | |
| Pop persistence No change | 0.13 – 1 | 0.58 | linear | 0.1 – 0.8 | -0.916 – 1 | 0.31 |
| Pop persistence CNRM-CM5, RCP 8.5 | 0.15 – 1 | 0.68 | linear | 0.1 – 0.8 | -0.87 – 1 | 0.62 |
| Pop persistence MIROC5, RCP 8.5 | 0.11 – 1 | 0.7 | linear | 0.1 – 0.8 | -0.98 – 1 | 0.67 |

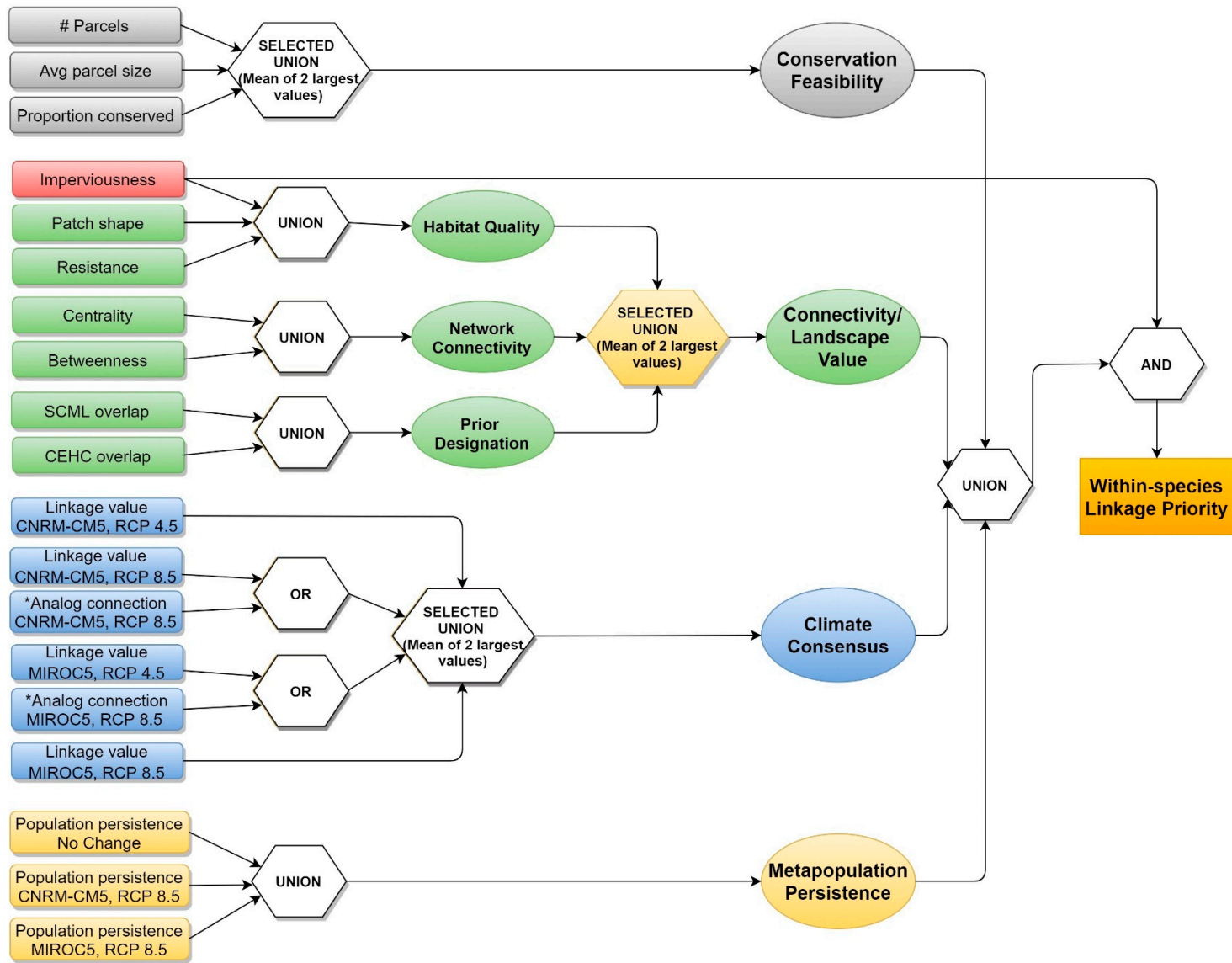


Figure S1. EEMS logic model for within-species linkage priority assessment.

Table S5. Input variables and processing approach to fuzzify variables for the within-species prioritization model depicted in Figure S1.

| Attribute | Description | Fuzzy Relationship | Combination 1 | Combination 2 | Combination 3 | Final Combination |
|----------------------------------|---|--------------------|---|---|---|--|
| # Parcels/Area | Number of parcels by patch area | Smaller = true | Mean of 2 most true = Conservation Feasibility | | Mean of <i>Conservation Feasibility</i> <i>Connectivity/Landscape Value</i> <i>Climate Consensus</i> & <i>Metapopulation Persistence</i> & <i>Metapopulation Persistence</i> | The smaller of <i>Imperviousness</i> and the mean of <i>Connectivity/Landscape Value</i> <i>Climate Consensus</i> & <i>Metapopulation Persistence</i> = Within-species Linkage Priority |
| Avg Parcel Size | Average parcel size within a segment | Larger = true | | | | |
| Proportion Conserved | Proportion of segment conserved | Larger = true | | | | |
| Imperviousness | Percent of impervious cover | Smaller = true | Mean = Habitat Quality | Mean of the 2 largest of the 3 values = Connectivity/Landscape Value | | |
| Patch Shape | Edge to interior ratio | Smaller = true | | | | |
| Resistance | Resistance as converted from habitat suitability for each species | Smaller = true | | | | |
| Centrality | Number of bordering patches | Larger = true | Mean = Network Connectivity | | | |
| Betweenness (log) | Number of neighboring patches that use node as a hub | Larger = true | | | | |
| SCML Overlap | Prop overlap with SC Missing Linkages | Larger = true | Mean = Prior Designation | | | |
| CEHC Overlap | Prop overlap with CA Essential Habitats Connectivity linkages | Larger = true | | | | |
| Linkage value, CNRM-CM5 RCP 4.5 | Prop of decades where linkage appears | Larger = true | Largest value carried forward | Mean of the 2 largest of 4 values = Climate Consensus | | |
| Linkage value, CNRM-CM5 RCP 8.5 | Prop of decades where linkage appears | Larger = true | | | | |
| CNRM-CM5, RCP 8.5 analog | Priority value based on climate analog | Larger = true | | | | |
| Linkage value, MIROC5 RCP 8.5 | Prop of decades where linkage appears | Larger = true | | | | |
| MIROC5, RCP 8.5 analog | Priority value based on climate analog | Larger = true | | | | |
| Linkage value, MIROC5 RCP 4.5 | Prop of decades where linkage appears | Larger = true | | | | |
| Pop persistence No Change | Linkage benefit - metapop model | Larger = true | Mean of values = Metapopulation Persistence | | | |
| Pop persistence CNRM-CM5 RCP 8.5 | Linkage benefit - metapop model | Larger = true | | | | |
| Pop persistence MIROC5 RCP 8.5 | Linkage benefit - metapop model | Larger = true | | | | |

S3: Metapopulation Modeling Maps

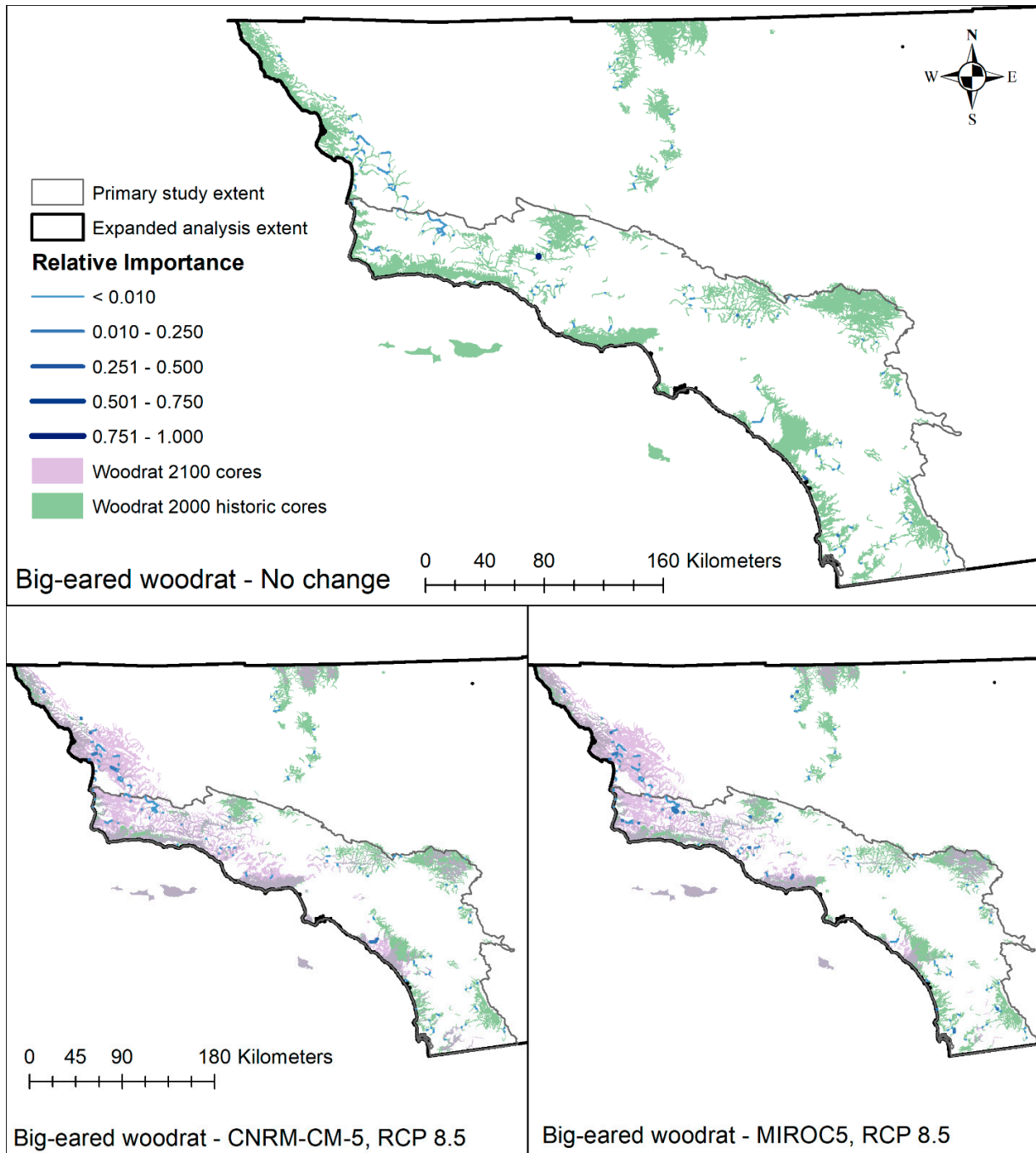


Figure S2. Maps of the relative importance values calculated for big-eared woodrat least cost paths with metapopulation models run from 2000 to 2100 under no change (top) as well as the CNRM-CM5 RCP 8.5 (bottom left) and MIROC5 RCP 8.5 future climate scenarios.

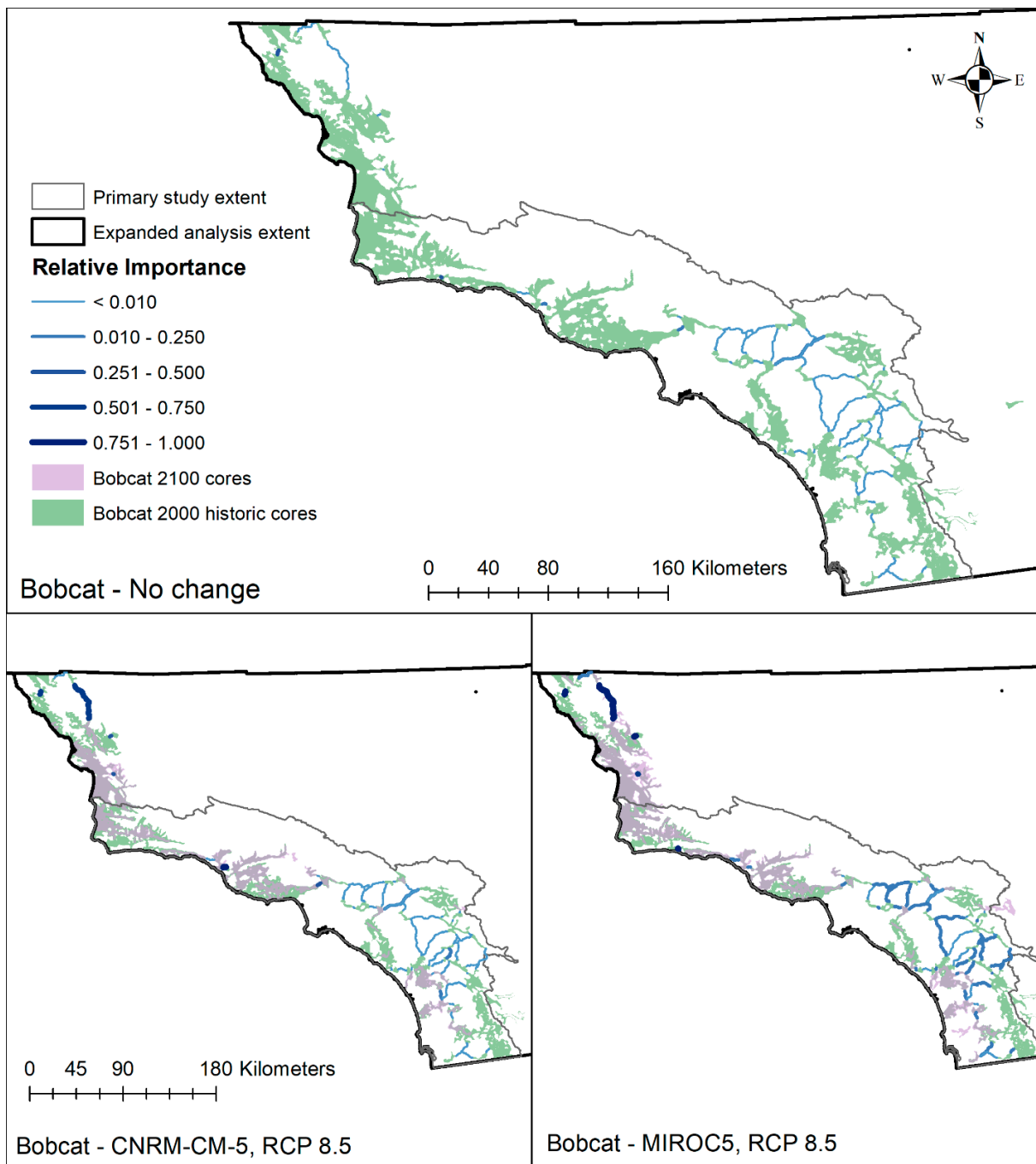


Figure S3. Maps of the relative importance values calculated for bobcat least cost paths with metapopulation models run from 2000 to 2100 under no change (top) as well as the CNRM-CM5 RCP 8.5 (bottom left) and MIROC5 RCP 8.5 future climate scenarios.

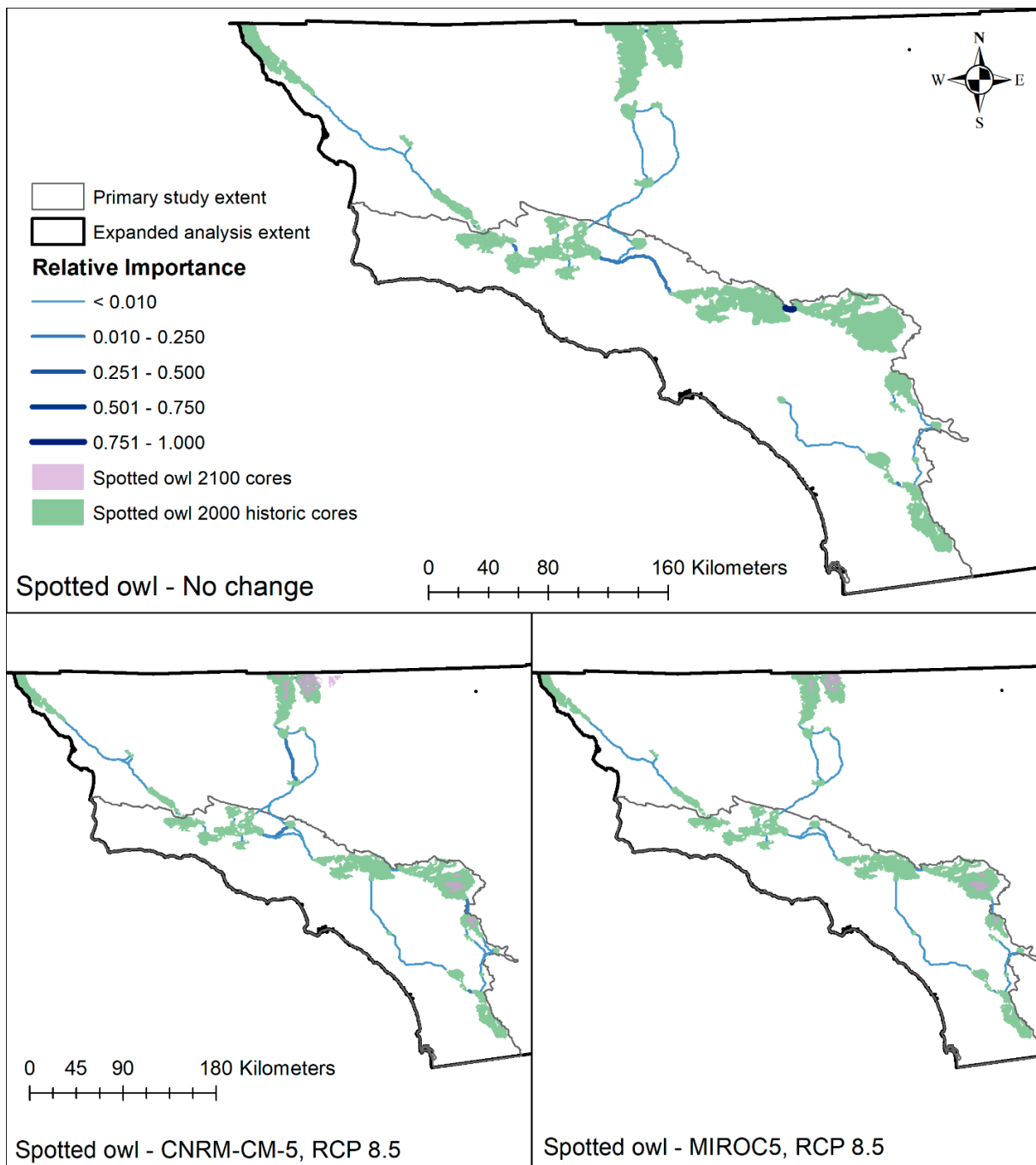


Figure S4. Maps of the relative importance values calculated for California spotted owl least cost paths with metapopulation models run from 2000 to 2100 under no change (top) as well as the CNRM-CM5 RCP 8.5 (bottom left) and MIROC5 RCP 8.5 future climate scenarios.

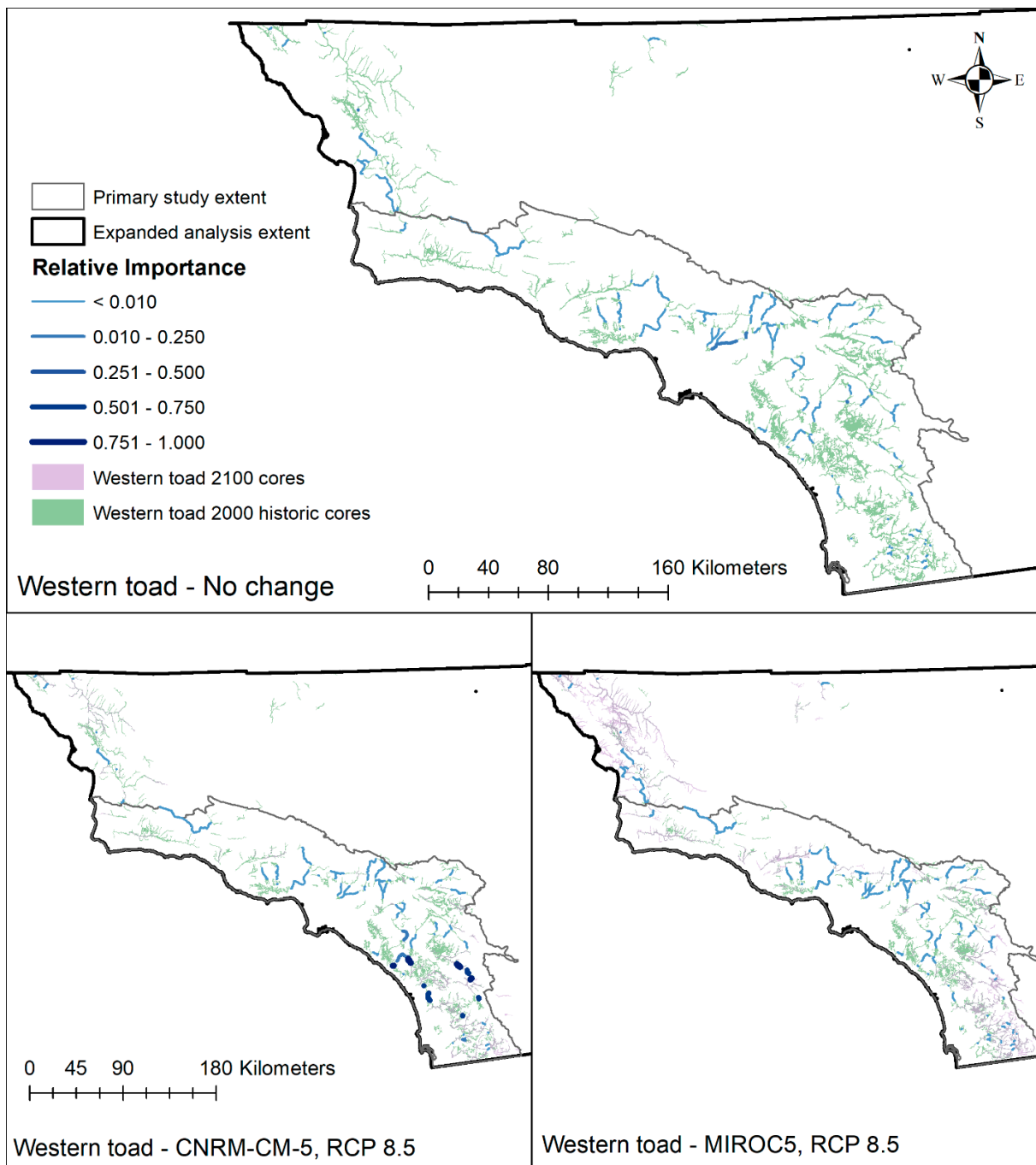


Figure S5. Maps of the relative importance values calculated for western toad least cost paths with metapopulation models run from 2000 to 2100 under no change (top) as well as the CNRM-CM5 RCP 8.5 (bottom left) and MIROC5 RCP 8.5 future climate scenarios.

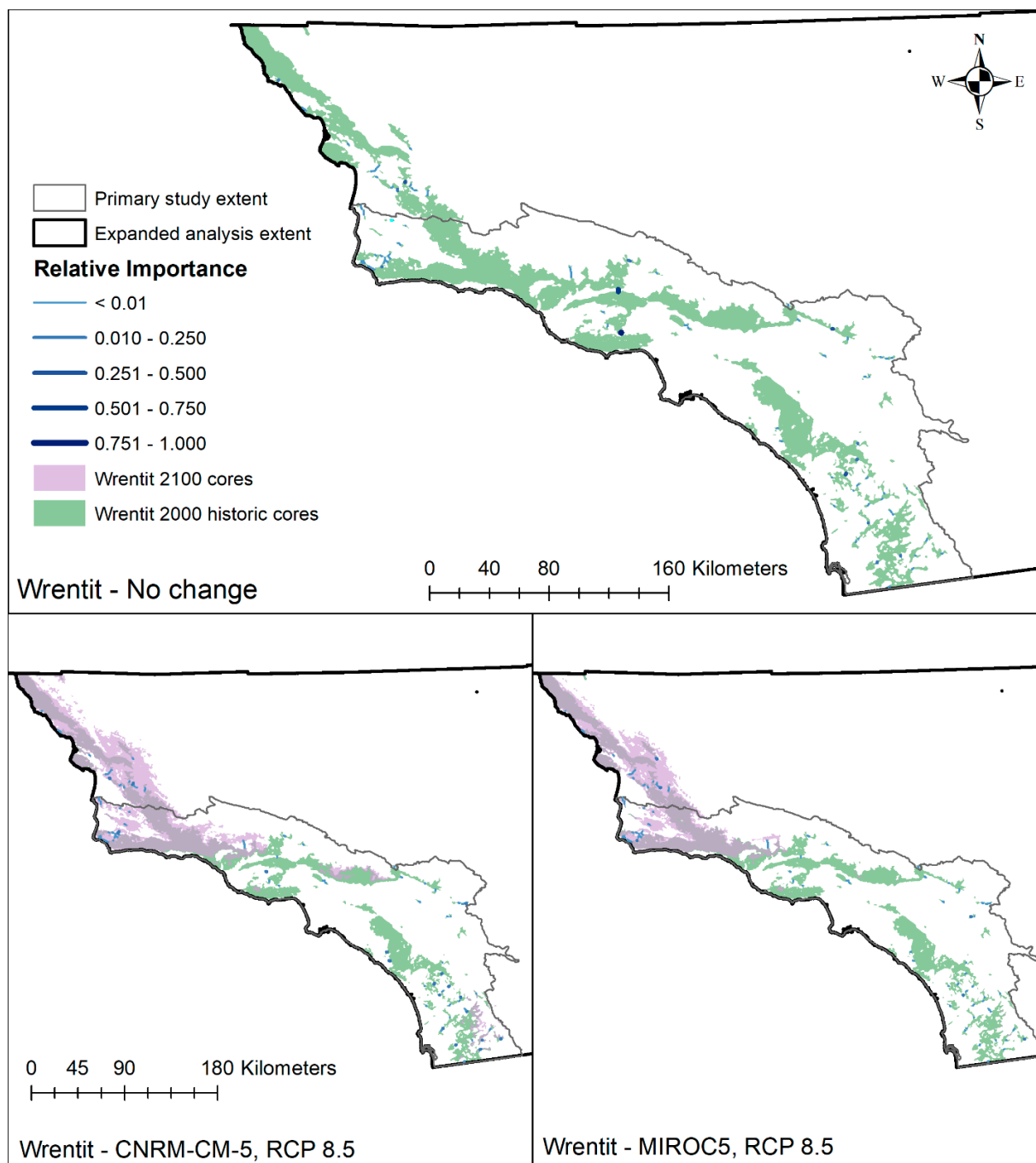


Figure S6. Maps of the relative importance values calculated for wren tit least cost paths with metapopulation models run from 2000 to 2100 under no change (top) as well as the CNRM-CM5 RCP 8.5 (bottom left) and MIROC5 RCP 8.5 future climate scenarios.

References

1. Phillips, S.J.; Anderson, R.P.; Schapire, R.E. Maximum entropy modeling of species geographic distributions. *Ecol. Modell.* **2006**, *190*, 231–259, doi:10.1016/j.ecolmodel.2005.03.026.

2. Franklin, J.; Wejnert, K.E.; Hathaway, S.A.; Rochester, C.J.; Fisher, R.N. Effect of species rarity on the accuracy of species distribution models for reptiles and amphibians in southern California. *Divers. Distrib.* **2009**, *15*, 167–177, doi:10.1111/j.1472-4642.2008.00536.x.
3. Barbet-Massin, M.; Jiguet, F.; Albert, C.H.; Thuiller, W. Selecting pseudo-absences for species distribution models: how, where and how many? *Methods Ecol. Evol.* **2012**, *3*, 327–338, doi:10.1111/j.2041-210X.2011.00172.x.
4. eBird eBird: An online database of bird distribution and abundance [web application] Available online: <http://www.ebird.org> (accessed on Jun 1, 2018).
5. California Department of Fish California Natural Diversity Database Available online: <https://www.wildlife.ca.gov/Data/CNDDDB> (accessed on Apr 17, 2017).
6. GBIF Global Biodiversity Information Facility occurrence download - *Anaxyrus boreas halophilus* Available online: <https://doi.org/10.15468/dl.hy8ykb> (accessed on Jun 1, 2018).
7. BISON Biodiversity Information Serving our Nation database Available online: <https://bison.usgs.gov/#home> (accessed on Apr 17, 2017).
8. U.S. Forest Service Natural Resource Inventory Database - Fauna.
9. HERP NA Herpetological Education and Research Project Available online: <http://www.naherp.com/> (accessed on Aug 14, 2018).
10. HerpMapper HerpMapper - A global herp atlas and data hub Available online: <http://www.herpMapper.org> (accessed on Jul 19, 2018).
11. GBIF Global Biodiversity Information Facility occurrence download - *Lynx rufus* Available online: <https://doi.org/10.15468/dl.iqs2jd> (accessed on Jun 4, 2018).
12. Arctos Actos occurrence database Available online: <https://arctosdb.org/> (accessed on May 22, 2016).
13. Tremor, S., Stokes, D., Spencer, W., Diffendorfer, J., Thomas, H., Chivers, S., Unitt, P. *San Diego County Mammal Atlas, 46th ed., Proceedings of the San Diego Society of Natural History*, , Eds., San Diego Natural History Museum, San Diego, CA, USA, 2017; ISBN 9780692895399.
14. Jennings, M.K.; Lewison, R.L. Planning for connectivity under climate change: Using bobcat movement to assess landscape connectivity across San Diego County's open spaces; San Diego, CA, USA, 2013.
15. GBIF Global Biodiversity Information Facility occurrence download - *Neotoma macrotis* Available online: <https://doi.org/10.15468/dl.2g6ava> (accessed on May 8, 2018).
16. VertNet VertNet database Available online: <http://vertnet.org/> (accessed on May 8, 2018).
17. Elith, J.; H. Graham, C.; P. Anderson, R.; Dudík, M.; Ferrier, S.; Guisan, A.; J. Hijmans, R.; Huetmann, F.; R. Leathwick, J.; Lehmann, A.; et al. Novel methods improve prediction of species' distributions from occurrence data. *Ecography (Cop.)*. **2006**, *29*, doi:10.1111/j.2006.0906-7590.04596.x.
18. Franklin, J.; Wejnert, K.E.; Hathaway, S.A.; Rochester, C.J.; Fisher, R.N. Effect of species rarity on the accuracy of species distribution models for reptiles and amphibians in southern California. *Divers. Distrib.* **2009**, *15*, 167–177, doi:10.1111/j.1472-4642.2008.00536.x.
19. Araújo, M.B.; New, M. Ensemble forecasting of species distributions. *Trends Ecol. Evol.* **2007**, *22*, 42–7, doi:10.1016/j.tree.2006.09.010.
20. Grenouillet, G.; Buisson, L.; Casajus, N.; Lek, S. Ensemble modelling of species distribution: the effects of geographical and environmental ranges. *Ecography (Cop.)*. **2011**, *34*, 9–17.
21. R Core Team R: A language and environment for statistical computing 2017.
22. Thuiller, W.; Georges, D.; Engler, R.; Breiner, F. biomod2: Ensemble Platform for Species Distribution Modeling. R package version 3.3-7 **2016**.
23. Hijmans, R.J.; Phillips, S.; Leathwick, J.; Elith, J. Package 'dismo' - Species Distribution Modeling.' *CRAN Repos.* **2017**.
24. Wood, S.N. Fast stable restricted maximum likelihood and marginal likelihood estimation of semiparametric generalized linear models. *J. R. Stat. Soc. Ser. B (Statistical Methodol.)* **2011**, *73*, 3–36, doi:10.1111/j.1467-9868.2010.00749.x.
25. Lobo, J.M.; Jiménez-Valverde, A.; Real, R. AUC: a misleading measure of the performance of predictive distribution models. *Glob. Ecol. Biogeogr.* **2008**, *17*, 145–151, doi:10.1111/j.1466-8238.2007.00358.x.

26. Allouche, O.; Tsoar, A.; Kadmon, R. Assessing the accuracy of species distribution models: Prevalence, kappa and the true skill statistic (TSS). *J. Appl. Ecol.* **2006**, *43*, 1223–1232, doi:10.1111/j.1365-2664.2006.01214.x.
27. Shirk, A.; McRae, B.H. Gnarly Landscape Utilities: Core Mapper user guide **2013**.
28. Keeley, A.T.H.; Beier, P.; Gagnon, J.W. Estimating landscape resistance from habitat suitability: effects of data source and nonlinearities. *Landscape Ecol.* **2016**, *31*, 2151–2162, doi:10.1007/s10980-016-0387-5.
29. Trainor, A.M.; Walters, J.R.; Morris, W.F.; Sexton, J.; Moody, A. Empirical estimation of dispersal resistance surfaces: A case study with red-cockaded woodpeckers. *Landscape Ecol.* **2013**, *28*, 755–767, doi:10.1007/s10980-013-9861-5.
30. Mateo-Sánchez, M.C.; Balkenhol, N.; Cushman, S.; Pérez, T.; Domínguez, A.; Saura, S. A comparative framework to infer landscape effects on population genetic structure: are habitat suitability models effective in explaining gene flow? *Landscape Ecol.* **2015**, *30*, 1405–1420, doi:10.1007/s10980-015-0194-4.
31. Comer, P.J.; Pressey, R.L.; Hunter, M.L.; Schloss, C.A.; Buttrick, S.C.; Heller, N.E.; Tirpak, J.M.; Faith, D.P.; Cross, M.S.; Shaffer, M.L. Incorporating geodiversity into conservation decisions. *Conserv. Biol.* **2015**, *29*, 692–701, doi:10.1111/cobi.12508.
32. Theobald, D.M.; Harrison-Atlas, D.; Monahan, W.B.; Albano, C.M. Ecologically-relevant maps of landforms and physiographic diversity for climate adaptation planning. *PLoS One* **2015**, *10*, doi:10.1371/journal.pone.0143619.
33. Beier, P.; Brost, B. Use of land facets to plan for climate change: Conserving the arenas, not the actors. *Conserv. Biol.* **2010**, *24*, 701–710, doi:10.1111/j.1523-1739.2009.01422.x.
34. Brost, B.M.; Beier, P. Use of land facets to design linkages for climate change. *Ecol. Appl.* **2012**, *22*, doi:10.1890/11-0213.1.
35. Jenness, J.; Brost, B.; Beier, P. Land facet corridor designer 2010. Available online: www.corridor-design.org (accessed on 15 May 2017).
36. Jenness, J.; Brost, B.; Beier, P. Land Facet Corridor Designer: Extension for ArcGIS. *Jenness Enterp.* **2013**, p. 110.
37. McRae, B.H.; Kavanagh, D.M. Linkage Mapper Connectivity Analysis Software 2011. Available online: <http://www.circuitscape.org/linkagemapper> (accessed on 15 May 2017).
38. Akçakaya, H.R.; Root, W.T. Linking landscape data with population viability analysis (Version 5.0) Applied Mathematics **2005**.
39. Salguero-Gómez, R.; Jones, O.R.; Archer, C.R.; Bein, C.; de Buhr, H.; Farack, C.; Gottschalk, F.; Hartmann, A.; Henning, A.; Hoppe, G.; et al. COMADRE: a global data base of animal demography. *J. Anim. Ecol.* **2016**, *85*, 371–384, doi:10.1111/1365-2656.12482.
40. Kelly, P.A. Population ecology and social organization of dusky-footed woodrats, *Neotoma fuscipes*, Ph.D. Dissertation, University of California, Berkeley, 1990; p. 382.
41. Linsdale, J.; Tevis, L.J. The dusky-footed woodrat: a record of observations made on the Hastings Natural History Reservation; University of California Press, 1951; p. 664.
42. Matocq, M.D. Reproductive success and effective population size in woodrats (*Neotoma macrotis*). *Mol. Ecol.* **2004**, *13*, 1635–1642, doi:10.1111/j.1365-294X.2004.02173.x.
43. Preston, K.L.; Rotenberry, J.T.; Redak, R.A.; Allen, M.F. Habitat shifts of endangered species under altered climate conditions: Importance of biotic interactions. *Glob. Chang. Biol.* **2008**, *14*, 2501–2515, doi:10.1111/j.1365-2486.2008.01671.x.
44. LaHaye, W.S.; Zimmerman, G.S.; Gutiérrez, R.J. Temporal variation in the vital rates of an insular population of spotted owls (*Strix occidentalis occidentalis*): Contrasting effects of weather. *Auk* **2004**, *121*, 1056–1069, doi:10.1093/auk/121.4.1056.
45. Baker, M.; Nur, N.; Geupel, G.R. Correcting biased estimates of dispersal and survival due to limited study area: Theory and an application using wrentits. *Condor* **1995**, *97*, 663–674, doi:10.2307/1369175.
46. Forsman, E.D.; Anthony, R.G.; Reid, J.A.; Loschl, P.J.; Sovern, S.G.; Taylor, M.; Biswell, B.L.; Ellingson, A.; Meslow, E.C.; Miller, G.S.; et al. Natal and breeding dispersal of northern spotted owls. *J. Wildl. Manage.* **2002**, *66*, 1–35, doi:10.2307/3830803.
47. Smith, M.H. Dispersal capacity of the dusky-footed woodrat, *Neotoma fuscipes*. *Am. Midl. Nat.* **1965**, *74*, 457, doi:10.2307/2423275.

48. Brehme, C.S.; Hathaway, S.A.; Fisher, R.N. An objective road risk assessment method for multiple species: ranking 166 reptiles and amphibians in California. *Landsc. Ecol.* **2018**, *33*, 911–935, doi:10.1007/s10980-018-0640-1.
49. Sheehan, T.; Gough, M. A platform-independent fuzzy logic modeling framework for environmental decision support. *Ecol. Inform.* **2016**, *34*, 92–101, doi:10.1016/j.ecoinf.2016.05.001.